Appl. Math. Mech. -Engl. Ed., **36**(10), 1305–1318 (2015)
DOI 10.1007/s10483-015-1985-9

Applied Mathematics and Mechanics (English Edition)

General investigation for longitudinal wave propagation under magnetic field effect via nonlocal elasticity*

U. GÜVEN†

Department of Mechanical Engineering, Yildiz Technical University,
Besiktas 34349, Turkey

Abstract In this paper, the propagation of longitudinal stress waves under a longitudinal magnetic field is addressed using a unified nonlocal elasticity model with two scale coefficients. The analysis of wave motion is mainly based on the Love rod model. The effect of shear is also taken into account in the framework of Bishop's correction. This analysis shows that the classical theory is not sufficient for this subject. However, this unified nonlocal elasticity model solely used in the present study reflects in a manner fairly realistic for the effect of the longitudinal magnetic field on the longitudinal wave propagation.

Key words Rayleigh-Bishop rod, nonlocal elasticity, magnetic field, wave propagation

Chinese Library Classification O353, O361
2010 Mathematics Subject Classification 74K10, 74B99, 74F15, 74J99

1 Introduction

Nowadays, the nanostructures, i.e., zero- (nano particles), one- (nanorods, nanowires, and nanobelts), and two-dimensional (thin films and nano sheets), have attracted great attention of many scientists and researchers. Due to the superior material properties and the smaller sizes, they also are candidates to new developing industrial applications. The subject of wave propagation in nanostructures are related closely with many crucial physical properties of them, such as electrical, optical conductance, and absorption coefficients. Especially, some recent notable studies done on the longitudinal wave propagation of the nanorods should be mentioned[1–4] here. Recently in years, in the studies done to reveal different magnetic properties of nanostructures elements, increasing efforts are observed. In this regard, some notable studies[5–13] related with the electronic and transport properties of nanotubes under a magnetic field have attracted considerable interest among the researchers. In relation to the present work, the investigations done to understand the effect of magnetic field on the wave propagation characteristics in the various structural elements having nano dimensions are crucial and may give the useful insights for the different applications in the nano-engineering field. As known from the literature[14], the vibrations of nanotubes are sensitive against changes of magnetic field. The applications of nanorods working in the magnetic field are diverse: bio magnetic sensors, solar cells, high density magnetic recording, microwave devices, tunable radio frequency oscillators, etc. The present open literature is rather rich for the works investigating the magnetic field effect on the transverse wave characteristics of nanostructures. Some notable previous works

* Received Dec. 24, 2014 / Revised Mar. 11, 2015
† Corresponding author, E-mail: uguven@yildiz.edu.tr

done relating with this topic have been quoted here. The effect of the longitudinal magnetic field on wave propagation in multi walled carbon nanotubes which can be viewed as a cylindrical shell embedded in elastic matrix was addressed[15] using the continuum medium theories. The effect of the longitudinal magnetic field on ultrasonic vibration in single walled carbon nanotubes which can be viewed as a cylindrical shell was investigated[16] using the nonlocal continuum medium theory. The effect of transverse magnetic field on dynamic characteristics of multi walled carbon nanotubes was reported[17]. The effect of the longitudinal magnetic field on wave propagation in a single walled carbon nanotube based on the nonlocal Euler-Bernoulli beam theory was presented[18]. The rigorous van der Waals interaction effect on vibration characteristics of multi-walled carbon nanotubes embedded in matrix under a transverse magnetic field was analytically investigated[19]. The influence of longitudinal magnetic field on the characteristics of both flexural and shear waves in a single walled carbon nanotube embedded in an elastic matrix was studied[20] by the nonlocal Rayleigh-Timoshenko and higher-order beam theories. Dynamic response of an embedded conducting nanowire subjected to an axial magnetic shock was investigated in the context of nonlocal continuum theory of Eringen[21]. The effect of the longitudinal magnetic field on the vibration of a magnetically sensitive double single walled carbon nanotube system which can be viewed as an equivalent nonlocal double Euler-Bernoulli beam system was reported[22]. Wave propagation in single-walled fluid-conveying carbon nanotubes in magnetic and temperature fields was studied[23] using a nonlocal Timoshenko beam model. Free vibrations and lateral instability of single walled carbon nanotubes subjected to three-dimensional magnetic fields were studied[24], where a nonlocal elasticity theory was incorporated into the classical Rayleigh beam theory. However, this analysis reported that the axial applied magnetic field has no effect on the phase velocity of longitudinal waves.

Despite numerous studies on analyzing transverse wave vibration of the nanostructures under magnetic field presence, the reports for longitudinal wave propagation still cannot be found, except a recent work[24]. The longitudinal magnetic field effect on the longitudinal wave propagation cannot be explained up to now by classical and various gradient elasticity models since these models are constructed in the absence of longitudinal magnetic field. The aim of the present theoretical analysis is to address accurately the effect of the longitudinal magnetic field on the longitudinal wave propagation along a nanorod. For this, firstly, developing a nonlocal elasticity model with the sufficient capacity is required. Therefore, in the present analysis, a unified nonlocal elasticity theory is incorporated into the classical Rayleigh (Love)-Bishop rod model[25]. Thus, lateral deformation effect and the contributions of shear stress components on the elastic strain energy are also taken into account in this analysis. The explicit solution obtained using Hamilton's principle is illustrated by some numerical examples. This work developed to reveal the effect of longitudinal magnetic field on the longitudinal wave propagation of the nanorods may be helpful particularly in the rational and optimum design of the nano electro-mechanical systems which can be used in different working fields.

2 Basic differential equations of motion

According to the basic hypotheses of Rayleigh (Love) rod theory, the displacement field in the Cartesian coordinates is expressed as

$$u = u(x,t), \quad v = -\nu y \frac{\partial u}{\partial x}, \quad w = -\nu z \frac{\partial u}{\partial x}, \tag{1}$$

where u, v, and w denote the x-, y-, and z-components of the displacement vector, respectively, and ν is Poisson's ratio. The x-axis is taken in the axial direction of the rod, and y and z denote the other perpendicular axes at the centre of geometry of the cross-section.

For the displacement field specified by Eq. (1), the strains and stresses are conventionally

obtained as follows:

$$\begin{cases} \varepsilon_{xx} = \dfrac{\partial u}{\partial x}, \quad \varepsilon_{yy} = \dfrac{\partial v}{\partial y} = -\nu\dfrac{\partial u}{\partial x}, \quad \varepsilon_{zz} = \dfrac{\partial w}{\partial x} = -\nu\dfrac{\partial u}{\partial x}, \quad \gamma_{xy} = \dfrac{\partial u}{\partial y} + \dfrac{\partial v}{\partial x} = -\nu y\dfrac{\partial^2 u}{\partial x^2}, \\ \gamma_{xz} = \dfrac{\partial w}{\partial x} + \dfrac{\partial u}{\partial z} = -\nu z\dfrac{\partial^2 u}{\partial x^2}, \quad \gamma_{yz} = \dfrac{\partial w}{\partial x} + \dfrac{\partial v}{\partial z} = 0, \end{cases} \tag{2}$$

$$\begin{cases} \sigma_{xx} = E\dfrac{\partial u}{\partial x}, \quad \sigma_{yy} = \sigma_{zz} = 0, \quad \tau_{xy} = -\dfrac{E}{2(1+\nu)}\nu y\dfrac{\partial^2 u}{\partial x^2}, \\ \tau_{xz} = -\dfrac{E}{2(1+\nu)}\nu z\dfrac{\partial^2 u}{\partial x^2}, \quad \tau_{yz} = 0, \end{cases} \tag{3}$$

where ε_{xx}, ε_{yy}, and ε_{zz} are the normal strains, γ_{xy}, γ_{xz}, and γ_{yz} are the shear strains, σ_{xx}, σ_{yy}, and σ_{zz} are the normal stresses, τ_{xy}, τ_{xz}, and τ_{yz} are the shear stresses, and E is the elasticity modulus.

The differential equations of the motion in the Cartesian coordinate system, taking into account the magnetic field presence, are expressed as follows[26]:

$$\frac{\partial \sigma_{xx}}{\partial x} + \frac{\partial \tau_{xy}}{\partial y} + \frac{\partial \tau_{xz}}{\partial z} + f_x = \rho\frac{\partial^2 u}{\partial t^2}, \tag{4}$$

$$\frac{\partial \tau_{yx}}{\partial x} + \frac{\partial \sigma_{yy}}{\partial y} + \frac{\partial \tau_{yz}}{\partial z} + f_y = \rho\frac{\partial^2 v}{\partial t^2}, \tag{5}$$

$$\frac{\partial \tau_{zx}}{\partial x} + \frac{\partial \tau_{zy}}{\partial y} + \frac{\partial \sigma_{zz}}{\partial z} + f_z = \rho\frac{\partial^2 w}{\partial t^2}, \tag{6}$$

where f_x, f_y, and f_z are the body force components along the x-, y-, and z-directions due to the longitudinal magnetic field effect. These components are given by[15–16,18]

$$f_x = 0, \tag{7}$$

$$f_y = \eta H_x^2\Big(\frac{\partial^2 v}{\partial x^2} + \frac{\partial^2 v}{\partial y^2} + \frac{\partial^2 w}{\partial y \partial z}\Big) = \eta H_x^2\frac{\partial^2 v}{\partial x^2}, \tag{8}$$

$$f_z = \eta H_x^2\Big(\frac{\partial^2 w}{\partial x^2} + \frac{\partial^2 w}{\partial y^2} + \frac{\partial^2 v}{\partial y \partial z}\Big) = \eta H_x^2\frac{\partial^2 w}{\partial x^2}, \tag{9}$$

where η is the magnetic permeability, and H_x is the component in the x-direction of the longitudinal magnetic field vector exerted on the nanorod.

3 Unified nonlocal elasticity model and general solution

The unified nonlocal elasticity model adopted here is a combination of the nonlocal integral (or Eringen)[27] and the strain gradient elasticity[28–32] models. Thus, the unified model has been proposed as[33–34]

$$(1 - l_{\mathrm{m}}^2\nabla^2)\sigma_{ij} = (1 - l_{\mathrm{s}}^2\nabla^2)(\lambda\delta_{ij}\varepsilon_{kk} + 2G\varepsilon_{ij}), \tag{10}$$

where l_{m} and l_{s} are the material constants in the nonlocal integral and the gradient elasticity models, respectively, λ and G are the Lamé constants, $\nabla^2 = (\frac{\partial^2}{\partial x^2} + \frac{\partial^2}{\partial y^2} + \frac{\partial^2}{\partial z^2})$ is the Laplacian operator, and δ_{ij} denotes the Kronecker delta. The nonlocal elasticity model of Eringen with $l_{\mathrm{s}} = 0$ removes only the strain singularity near the dislocation core region, while the gradient elasticity model with $l_{\mathrm{m}} = 0$ removes only the strain singularity near the dislocation core

region. However, both the strain and stress singularities near the dislocations are removed by this unified nonlocal elasticity model with two scale coefficients. It has been reported[34] that this unified nonlocal elasticity model can give a wider conclusion based on the experimental observations, when compared with the conventional nonlocal elasticity theory. Furthermore, it has been shown[35] that there is an excellent matching between the dispersive curve of the Born-Karman model with this unified nonlocal elasticity model.

By Eqs. (4)–(10) and after a few simple derivative operations, the existing stress components are obtained as

$$\sigma_{xx} = \rho(1+2\nu)l_{\mathrm{m}}^2\frac{\partial^3 u}{\partial x\partial t^2} - 2\nu\eta H_x^2 l_{\mathrm{m}}^2\frac{\partial^3 u}{\partial x^3} + E\frac{\partial u}{\partial x} - El_{\mathrm{s}}^2\frac{\partial^3 u}{\partial x^3}, \tag{11}$$

$$\tau_{xy} = -\nu\rho y l_{\mathrm{m}}^2\frac{\partial^4 u}{\partial x^2\partial t^2} + \nu y\eta H_x^2 l_{\mathrm{m}}^2\frac{\partial^4 u}{\partial x^4} - \frac{E}{2(1+\nu)}\nu y\frac{\partial^2 u}{\partial x^2} + \frac{E}{2(1+\nu)}\nu y l_{\mathrm{s}}^2\frac{\partial^4 u}{\partial x^4}, \tag{12}$$

$$\tau_{xz} = -\nu\rho z l_{\mathrm{m}}^2\frac{\partial^4 u}{\partial x^2\partial t^2} + \nu z\eta H_x^2 l_{\mathrm{m}}^2\frac{\partial^4 u}{\partial x^4} - \frac{E}{2(1+\nu)}\nu z\frac{\partial^2 u}{\partial x^2} + \frac{E}{2(1+\nu)}\nu z l_{\mathrm{s}}^2\frac{\partial^4 u}{\partial x^4}. \tag{13}$$

In the present analysis, the governing equation of longitudinal wave motion is deduced from the application of Hamilton's principle. Thus, firstly, the total elastic strain energy U, considering the contribution of the shear stress components, is calculated as follows[36–41]:

$$U = \frac{1}{2}\iiint(\sigma_{xx}\varepsilon_{xx} + \tau_{xy}\gamma_{xy} + \tau_{xz}\gamma_{xz})\mathrm{d}V. \tag{14}$$

Substituting Eqs. (11)–(13) into Eq. (14), the total elastic strain energy expression becomes as follows:

$$\begin{aligned} U = \frac{1}{2}\int_0^L \Big(&\rho(1+2\nu)AL_{\mathrm{m}}^2\frac{\partial u}{\partial x}\frac{\partial^3 u}{\partial x\partial t^2} + EA\Big(\frac{\partial u}{\partial x}\Big)^2 - EAl_{\mathrm{s}}^2\frac{\partial u}{\partial x}\frac{\partial^3 u}{\partial x^3} - 2\nu A\eta H_x^2 l_{\mathrm{m}}^2\frac{\partial u}{\partial x}\frac{\partial^3 u}{\partial x^3} \\ &+ \rho\nu^2 I_{\mathrm{p}} l_{\mathrm{m}}^2\frac{\partial^2 u}{\partial x^2}\frac{\partial^4 u}{\partial x^2\partial t^2} + \frac{E}{2(1+\nu)}\nu^2 I_{\mathrm{p}}\Big(\frac{\partial^2 u}{\partial x^2}\Big)^2 - \frac{E}{2(1+\nu)}\nu^2 I_{\mathrm{p}} l_{\mathrm{s}}^2\frac{\partial^2 u}{\partial x^2}\frac{\partial^4 u}{\partial x^4} \\ &- \nu^2 I_{\mathrm{p}}\eta H_x^2 l_{\mathrm{m}}^2\frac{\partial^2 u}{\partial x^2}\frac{\partial^4 u}{\partial x^4}\Big)\mathrm{d}x, \end{aligned} \tag{15}$$

where A and I_{p} are the cross-sectional area and the second polar moment, respectively.

The kinetic energy T is given by

$$T = \frac{1}{2}\rho\iiint(\dot{u}^2 + \dot{v}^2 + \dot{w}^2)\mathrm{d}V, \tag{16}$$

where dot sign denotes the derivative with respect to time.

When considering the displacement field (1), the potential energy expression becomes as follows:

$$T = \frac{1}{2}\int_0^L \Big(\rho A\Big(\frac{\partial u}{\partial t}\Big)^2 + \rho\nu^2 I_{\mathrm{p}}\Big(\frac{\partial^2 u}{\partial x\partial t}\Big)^2\Big)\mathrm{d}x. \tag{17}$$

The general expression of the work done by body forces is given by[36]

$$W_{\mathrm{b}} = \iiint f_i u_i \mathrm{d}V, \tag{18}$$

where f_i denotes the body force components, and u_i denotes the displacement components. The contribution of this work for the present problem is absent ($W_{\mathrm{b}} = \iiint f_x u\mathrm{d}V = 0$).

Hamilton's principle can be expressed as

$$\delta \int_{t_1}^{t_2} (T-U)\mathrm{d}t = 0. \tag{19}$$

By substituting Eqs. (15) and (16) for U and T, respectively, into Eq. (19), the governing equation of motion is obtained as

$$\begin{aligned}
&-\rho A\frac{\partial^2 u}{\partial t^2} + EA\frac{\partial^2 u}{\partial x^2} - \frac{E\nu^2 I_\mathrm{p}}{2(1+\nu)}\frac{\partial^4 u}{\partial x^4} + \rho\nu^2 I_\mathrm{p}\frac{\partial^4 u}{\partial x^2\partial t^2} + l_\mathrm{m}^2\Big(\rho(1+2\nu)A\frac{\partial^4 u}{\partial x^2\partial t^2} - \rho\nu^2 I_\mathrm{p}\frac{\partial^6 u}{\partial x^4\partial t^2}\Big)\\
&+ l_\mathrm{s}^2\Big(\frac{E\nu^2 I_\mathrm{p}}{2(1+\nu)}\frac{\partial^6 u}{\partial x^6} - EA\frac{\partial^4 u}{\partial x^4}\Big) - 2\nu A\eta H_x^2 l_\mathrm{m}^2\frac{\partial^4 u}{\partial x^4} + \nu^2 I_\mathrm{p}\eta H_x^2 l_\mathrm{m}^2\frac{\partial^6 u}{\partial x^6} = 0
\end{aligned} \tag{20}$$

together with the associated boundary conditions

$$\begin{aligned}
&\Big(-EA\frac{\partial u}{\partial x} + (l_\mathrm{s}^2 EA + 2l_\mathrm{m}^2\nu A\eta H_x^2 + G\nu^2 I_\mathrm{p})\frac{\partial^3 u}{\partial x^3} - (l_\mathrm{s}^2 G\nu^2 I_\mathrm{p} + l_\mathrm{m}^2\nu^2 I_\mathrm{p}\eta H_x^2)\frac{\partial^5 u}{\partial x^5}\\
&- (l_\mathrm{m}^2(1+2\nu)\rho A + \rho\nu^2 I_\mathrm{p})\frac{\partial^3 u}{\partial x\partial t^2} + l_\mathrm{m}^2\rho\nu^2 I_\mathrm{p}\frac{\partial^5 u}{\partial x^3\partial t^2}\Big)|\delta u|_0^L\\
&+ \Big(-(G\nu^2 I_\mathrm{p} + \frac{1}{2}(l_\mathrm{s}^2 EA + 2l_\mathrm{m}^2\nu A\eta H_x^2))\frac{\partial^2 u}{\partial x^2}\\
&+ (l_\mathrm{s}^2 G\nu^2 I_\mathrm{p} + l_\mathrm{m}^2\nu^2 I_\mathrm{p}\eta H_x^2)\frac{\partial^4 u}{\partial x^4} - l_\mathrm{m}^2\nu^2\rho I_\mathrm{p}\frac{\partial^4 u}{\partial x^2\partial t^2}\Big)|\delta u'|_0^L\\
&+ \Big(\frac{1}{2}(l_\mathrm{s}^2 EA + 2l_\mathrm{m}^2\nu A\eta H_x^2)\frac{\partial u}{\partial x} - \frac{1}{2}(l_\mathrm{s}^2 Gv^2 I_\mathrm{p} + l_\mathrm{m}^2\nu^2 I_\mathrm{p}\eta H_x^2)\frac{\partial^3 u}{\partial x^3}\Big)|\delta u''|_0^L\\
&+ \Big(\frac{1}{2}(l_\mathrm{s}^2 Gv^2 I_\mathrm{p} + l_\mathrm{m}^2\nu^2 I_\mathrm{p}\eta H_x^2)\frac{\partial^2 u}{\partial x^2}\Big)|\delta u'''|_0^L\\
&= 0,
\end{aligned} \tag{21}$$

where $()'$ represents the derivative with respect to x.

In this investigation, the harmonic longitudinal wave propagation in the axial direction is assumed. Therefore, its propagation can be expressed in the complex form as follows:

$$u = \widetilde{U}\mathrm{e}^{\mathrm{i}k(x-ct)}, \tag{22}$$

where k denotes the wave number, c is the phase velocity, and $\widetilde{U}$ is the wave amplitude. Substituting Eq. (22) into Eq. (20), the corresponding general solution for the phase velocity is obtained in the dimensionless form as follows:

$$c^* = \sqrt{\frac{1 + \frac{\nu^2 r_0^2 k^2}{2(1+\nu)} + l_\mathrm{m}^2 k^2\frac{\eta H_x^2}{E}(2\nu + \nu^2 r_0^2 k^2) + l_\mathrm{s}^2 k^2(1 + \frac{\nu^2 r_0^2 k^2}{2(1+\nu)})}{1 + \nu^2 r_0^2 k^2 + l_\mathrm{m}^2 k^2(1 + 2\nu + \nu^2 r_0^2 k^2)}}, \tag{23}$$

where $c^* = \frac{c}{c_0}$, $c_0 = \frac{E}{\rho}$, and the gyration radius $r_0 = \sqrt{\frac{I_\mathrm{p}}{A}}$. For a solid rod with the radius a, r_0 is $a/\sqrt{2}$.

The group velocity c_g is given as follows:

$$c_\mathrm{g} = c_0\sqrt{\frac{A}{B}} + \frac{1}{2}c_0 k\frac{1}{\sqrt{\frac{A}{B}}}\frac{A'B - B'A}{B^2}, \tag{24}$$

where

$$A = 1 + \frac{\nu^2 r_0^2 k^2}{2(1+\nu)} + l_{\mathrm{m}}^2 k^2 \frac{\eta H_x^2}{E}(2\nu + \nu^2 r_0^2 k^2) + l_{\mathrm{s}}^2 k^2 \Big(1 + \frac{\nu^2 r_0^2 k^2}{2(1+\nu)}\Big),$$
$$B = 1 + \nu^2 r_0^2 k^2 + l_{\mathrm{m}}^2 k^2 (1 + 2\nu + \nu^2 r_0^2 k^2),$$

and $(\,)'$ prime denotes derivative with respect to the wave number k.

4 Degenerate cases and numerical results

For $l_{\mathrm{s}} = 0$, the general solution (23) is reduced to the degenerate case based on Eringen's integral approach in the following form:

$$c^* = \sqrt{\frac{1 + \frac{\nu^2 r_0^2 k^2}{2(1+\nu)} + l_{\mathrm{m}}^2 k^2 \frac{\eta H_x^2}{E}(2\nu + \nu^2 r_0^2 k^2)}{1 + \nu^2 r_0^2 k^2 + l_{\mathrm{m}}^2 k^2 (1 + 2\nu + \nu^2 r_0^2 k^2)}}. \tag{25}$$

The terms containing the following forms: $\frac{\nu^2 r_0^2 k^2}{2(1+\nu)}$ and 2ν. When these two are removed, the general solution (25) is reduced to the degenerate case based on the nonlocal Love rod theory in the following form:

$$c_{\mathrm{L}}^* = \sqrt{\frac{1 + l_{\mathrm{m}}^2 k^2 \frac{\eta H_x^2}{E} \nu^2 r_0^2 k^2 + l_{\mathrm{s}}^2 k^2}{(1 + l_{\mathrm{m}}^2 k^2)(1 + \nu^2 r_0^2 k^2)}}. \tag{26}$$

For $l_{\mathrm{s}} = H_x = 0$, Eq. (24) is reduced to the nonlocal Love rod solution (without the magnetic field effect) derived by the different way[42].

For short wavelengths (i.e., $k \to \infty$), the general dispersion relation (23) is reduced to the following form:

$$c^* = \sqrt{\frac{\eta H_x^2}{E} + \Big(\frac{l_{\mathrm{s}}}{l_{\mathrm{m}}}\Big) \frac{1}{2(1+\nu)}}. \tag{27}$$

For $k \to \infty$, Eqs. (25) and (26) give the same results as follows:

$$c^* = c_{\mathrm{L}}^* = \sqrt{\frac{\eta H_x^2}{E}}. \tag{28}$$

Comparing the relations (25) and (26), the superiority of the present model can be understood clearly. It can be seen in the above that while the nonlocal elasticity theory of Eringen gives the solution independent of the shear and scale coefficients influences, the present unified general model gives a physically realistic solution containing these effects for the phase velocity.

Figure 1(a) shows the effect of length scale parameter ratio $m = l_{\mathrm{s}}/l_{\mathrm{m}}$ on the phase velocity based on the present model, where ka, c^* $(= \frac{c}{c_0})$, and $H = \frac{\eta H_x^2}{E}$ are the dimensionless wave number, the dimensionless phase velocity, and the dimensionless parameter reflecting the effect of magnetic field, respectively. In calculations, l_{m} and H are taken to be 0.1 and 0.5, respectively. It is seen from Fig. 1(a) that the phase velocity always increases with the increase in the scale coefficient ratio m, and then for sufficiently high values of the wave number, the dispersion curves become asymptotic. It means that the stiffening capability of the longitudinal magnetic field on the nanorod occurs in smaller wave numbers for high values of the ratio m. Figure 1(b) depicts the effects of the ratio of scale coefficients m on the dispersion curves without the magnetic field. A simple comparison between Figs. 1(a) and (b) shows that the presence of the longitudinal magnetic field has a significant structural stiffening capability.

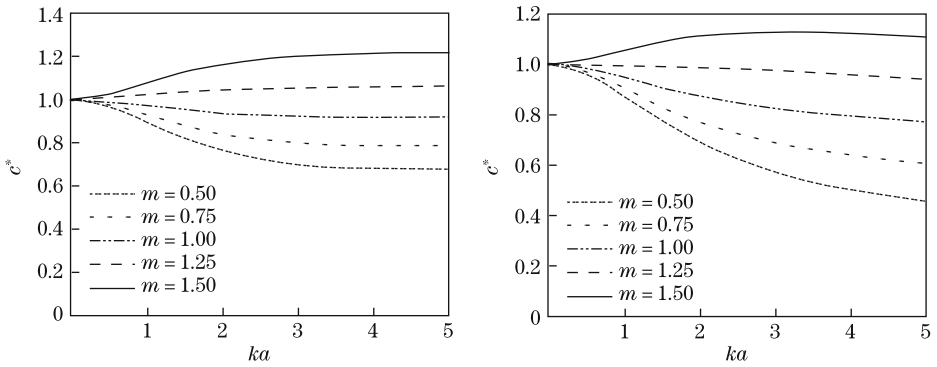

(a) Strong magnetic field ($H = 0.5$) (b) Without magnetic field ($H = 0.0$)

Fig. 1 Variation of phase velocity versus wave number for different ratios of scale coefficients m

Figure 2 illustrates the effect of shear on the phase velocity comparing the present and nonlocal Love solutions for $l_{\mathrm{s}} = 0$, where c_{ps} is the present solution, and c_{nL} is the nonlocal Love solution. Figure 2 shows that the shear effect increases with the increase in H, and for high values of the wave number, the increase is more significant.

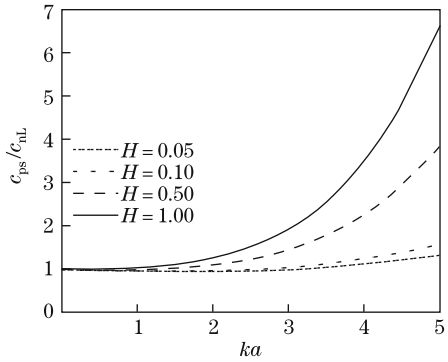

Fig. 2 Comparison of present Rayleigh-Bishop and nonlocal Love solutions under different magnetic fields for $l_{\mathrm{s}} = 0$

Figure 3 shows the variation of phase velocity with short wavelengths versus m for different values of H. It is seen that the limit phase velocity increases with the increase in m and H. It must be noticed that the limit phase velocity variation versus the parameter m, in the small values of parameter H, is more significant. In all numerical calculations, Poisson's ratio ν is taken to be 1/4, except Fig. 12.

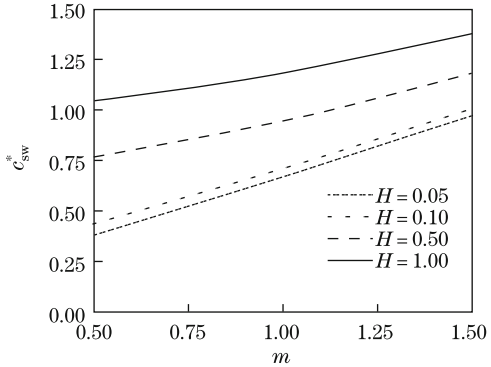

Fig. 3 Variation of phase velocity with short wavelength (c^*_{sw}) versus ratio of scale coefficients m under different magnetic field intensities H

The variation of phase velocity c^* based on the generalized nonlocal integral model versus the dimensionless wave number for two different scale parameters and magnetic fields intensities is depicted in Fig. 4. It can be seen from Fig. 4 that the phase velocity always increases with the increase in the magnetic field intensity H and with the decrease in the scale coefficient l_{m}. The increase seen in the phase velocity with the increase in the intensity of magnetic field becomes more evident when increasing the values of scale coefficients.

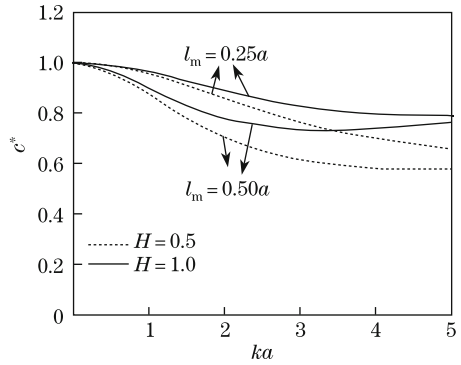

Fig. 4 Variation of phase velocity based on present solution versus wave number in strong magnetic fields for two different scale coefficients l_{m}

The variation of the ratio of velocities c_{g}/c versus the dimensionless wave number ka without the magnetic field is depicted in Fig. 5. The ratio of velocities, i.e., group and phase, continuously decreases as can be seen from Fig. 5, and this decrease becomes quicker with the increase in the value of scale coefficient. In this case, since the ratio c_{g}/c is always less than 1, the dispersion relation is called the normal dispersion[43]. Furthermore, it is seen that the group velocity approaches zero with increasing the values of the wave number ka. Moreover, the group velocity becomes zero in smaller values of the wave number ka with increasing the scale coefficient l_{m}.

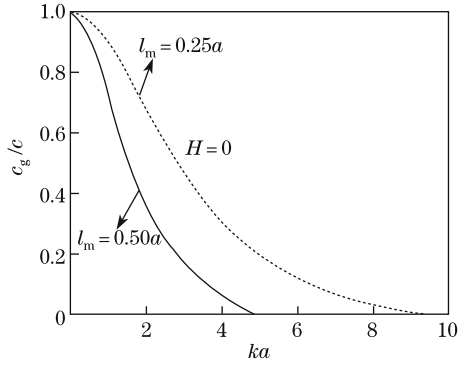

Fig. 5 Variation of ratio of group and phase velocities versus wave number without magnetic field for two different scale coefficients l_{m}

The variation of the ratio c_{g}/c versus the wave number ka under a weak magnetic field is depicted in Fig. 6. It is seen that the variations of curves are insensitive to the magnetic field intensity variation in its current intensity range for sufficiently small wave number (e.g., < 2) values. Comparing Fig. 5 with Fig. 6, it can be clearly seen that the variations of curves

depending on the magnetic field presence are significantly different. The structural stiffening capability of longitudinal magnetic field becomes more evident with increasing the wave number ka and the scale coefficient l_{m} as can be seen from Fig. 6. However, since the ratio c_{g}/c is always less than 1, the characteristic of the longitudinal wave is the normal dispersion in the current range, as previously indicated.

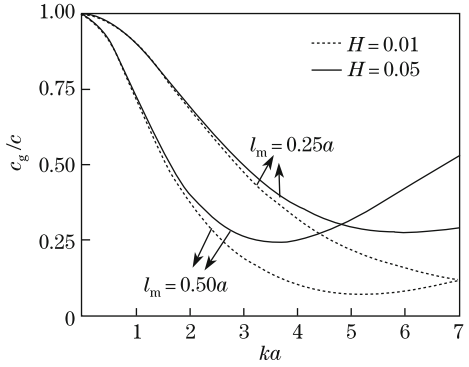

Fig. 6 Variation of ratio of group and phase velocities versus wave number under two different weak magnetic fields for two different values of scale coefficients

The variation of the ratio c_{g}/c versus the wave number ka under a strong magnetic field is depicted in Fig. 7. It is seen that for higher values of ka, the scale coefficient becomes $c_{\mathrm{g}}/c > 1$ under a strong magnetic field. Therefore, the characteristics of longitudinal wave become abnormal dispersion at specific intervals.

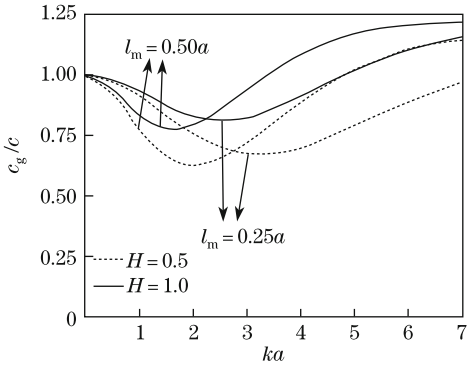

Fig. 7 Variation of ratio of group and phase velocities versus wave number under two different strong magnetic fields for two different values of scale coefficients l_{m}

The variation of the ratio c_{g}/c versus the dimensionless wave number ka under a weak magnetic field for different values of $m\,(= l_{\mathrm{s}}/l_{\mathrm{m}})$ is depicted in Fig. 8. The ratio c_{g}/c increases with the increase in m, as can be seen from Fig. 8. However, the ratio c_{g}/c is always smaller than 1.

The same variation is shown in Fig. 9 for $H = 0.5$. It is seen that the ratio c_{g}/c is nearly 1 in a current range of the dimensionless wave number ka, i.e., the wave characteristic becomes quasi non-dispersive for $m = 1$.

The variation of the ratio c_{g}/c with the wave number ka for $H = 1$ is depicted in Fig. 10. It can be seen that the wave characteristics becomes abnormal (i.e., $c_{\mathrm{g}}/c > 1$) for sufficient high

values of ka (e.g., > 4) and in all present values of m. With the increase in the ratio m under the strong magnetic field, the ratio becomes $c_g/c > 1$. A comparison between Figs. 8–10 shows that the longitudinal magnetic field intensity has a dominant effect on the wave characteristics (i.e., abnormal dispersive or normal dispersive).

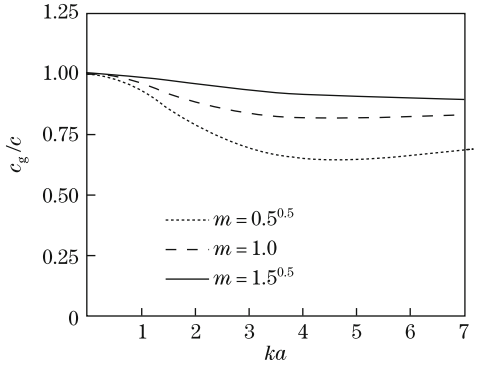

Fig. 8 Variation of ratio of group and phase velocities versus wave number under different values of ratio of scale coefficients m for $H = 0.01$

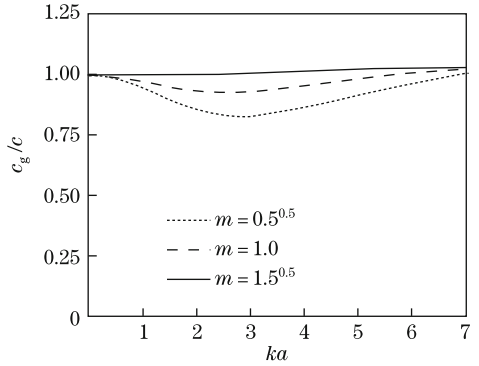

Fig. 9 Variation of ratio of group and phase velocities versus wave number under different values of ratio of scale coefficients m for $H = 0.5$

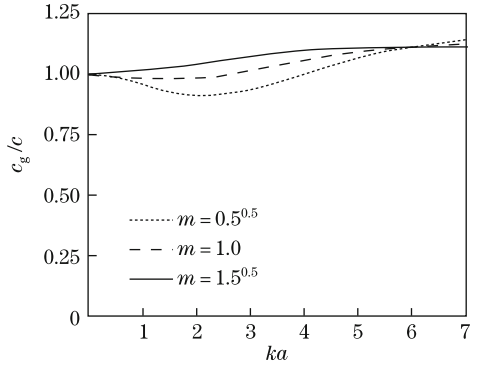

Fig. 10 Variation of ratio of group and phase velocities versus wave number under different values of ratio of scale coefficients m for $H = 1$

In Figs. 11 and 12, the current nonlocal Love rod solution including the magnetic field effect is compared with the nonlocal Love rod solution without the magnetic field effect that was developed by Narendar[42]. Figure 11 shows the magnetic field effect on the dispersion curves of the nanotubes for different mean radii $r_{\text{mean}} = 1\,\text{nm}$ and $5\,\text{nm}$. In numerical calculations, $H = 0.1$, $\nu = 0.12$[44], and the nonlocal scale coefficient $l_{\text{m}} = 0.1$. Figure 11 reveals that the magnetic field effect on the frequencies f is almost absent, for the sufficiently small wave numbers, and by the decrease in the nanotube radius, the magnetic field effect appears in higher wave numbers. Furthermore, the magnetic field effect on the frequencies becomes more

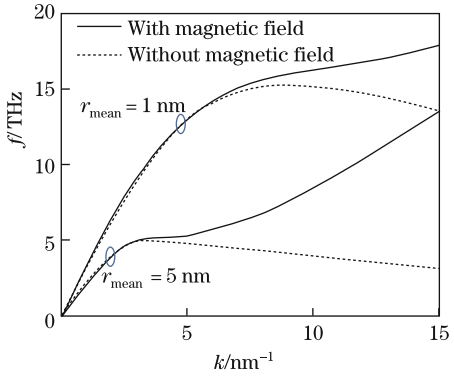

Fig. 11 Longitudinal magnetic field effect on variation of frequency versus wave number of nonlocal Love nanotube for two different radii

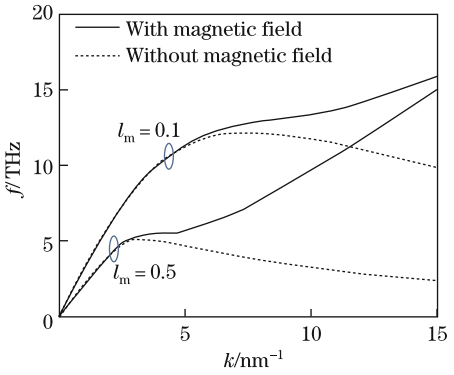

Fig. 12 Longitudinal magnetic field effect on variation of frequency versus wave number of nonlocal Love nanorod for two different scale coefficients

meaningful, for the high radii, especially in the values of high wave numbers.

The relationship between the nonlocal scale coefficient and the magnetic field capability is addressed in Fig. 12. In numerical calculations, $H = 0.1$, the nanorod radius is 1 nm, and $l_{\text{m}} = 0.1\,\text{nm}$ and $0.5\,\text{nm}$. It can be seen from Fig. 12 that the magnetic field effect on the frequencies is almost absent for sufficiently small wave numbers, and the magnetic field effect appears in higher wave numbers due to the decrease in the nanorod radius. Furthermore, the magnetic field effect on the frequencies becomes more meaningful for high scale coefficients, especially in the values of high wave numbers.

Unfortunately, experimental or molecular dynamic studies to check correctness of the present results are unavailable in the open literature. Also, as far as known in the open literature, no previous studies are available investigating the effect of longitudinal magnetic field on the nonlocal longitudinal wave propagation including inertia and shear effects. Therefore, a direct comparison of the analysis cannot be made. However, the present analysis reveals that the phase velocity decreases with the increase in the scale coefficient. This result is compatible with a recent study[24] done in the literature on carbon nanotubes. Moreover, it has been reported[24] that the presence of the longitudinal magnetic field has no effect on the phase velocity of longitudinal waves. This analytical finding constitutes a powerful support of the present analysis.

5 Conclusions

In the present work, to investigate the characteristics of longitudinal wave propagation along a nanorod subjected to the longitudinal magnetic field, a new nonlocal elasticity model is developed. To this end, a unified nonlocal elasticity theory with two scale coefficients is incorporated into the classical Rayleigh (Love)-Bishop rod model. As indicated previously

in the introduction section, the effect of longitudinal magnetic field on the longitudinal wave propagation cannot be explained up to now by classical and various gradient elasticity models, since these models do not contain the longitudinal magnetic field. The present analysis shows that the dispersion relation based on the nonlocal elasticity model of Eringen (i.e., $l = 0$) does not contain the influence of scale coefficients in the limiting case with short wave lengths. For this reason, the phase velocities for short wavelengths seem independent of the shear effect. Secondly, the present analysis clearly shows that the dispersion relation obtained by the strain gradient elasticity model (i.e., $l_{\mathrm{m}} = 0$) does not reflect the influence of the longitudinal magnetic field. Hence, the nonlocal second- and fourth-order strain gradient models[2] for an ultrasonic wave dispersion analysis of a nanorod cannot be used in this paper. Similarly, the nonlocal elasticity theories obtained by incorporating the classical Rayleigh[24] or Bernoulli-Euler[1–4] beam models cannot be used for the present analysis. Moreover, it should be seen that any information regarding the influence of the longitudinal magnetic field cannot be obtained for the present analysis using the classical Rayleigh (Love)-Bishop rod model. As a final statement, this work gives reliable and sensitive results for the characteristics of longitudinal wave in a nanorod under a longitudinal magnetic field using a new consistent nonlocal elasticity model. The successful technological applications of various nanostructures are closely related with their physical properties determining sensitively. Thus, this analysis can be hopefully expected to be useful, for the rational and optimal design of the nano electro-mechanical structures.

References

[1] Narendar, S. and Gopalkrishnan, S. Nonlocal scale effects on ultrasonic wave characteristics of nanorods. *Physica E-Low-Dimensional Systems and Nanostructures*, **42**, 1601–1604 (2010)

[2] Narendar, S. Ultrasonic wave characteristics of nanorods via nonlocal strain gradient models. *Journal of Applied Physics*, **107**, 084312 (2010)

[3] Narendar, S. and Gopalkrishnan, S. Axial wave propagation in coupled nanorod system with nonlocal small scale effects. *Composites Part B-Engineering*, **42**, 2013–2023 (2011)

[4] Murmu, T. and Adhikari, S. Nonlocal effects in the longitudinal vibration of double-nanorod systems. *Physica E-Low-Dimensional Systems and Nanostructures*, **43**, 415–422 (2010)

[5] Li, T. S. and Lin, M. F. Transport properties of finite carbon nanotubes under electric and magnetic fields. *Journal of Physica Condensed Matter*, **18**, 10693–10703 (2006)

[6] Rosales, L., Pacheco, M., Barticevic, Z., Rocha, C. G., and Latgé, A. Magnetic-field effects on transport in carbon nanotube junctions. *Physical Review B*, **75**, 165401 (2007)

[7] Belluci, S., Gonzalez, J., Guinea, F., Onorato, P., and Perfetto, E. Magnetic field effects in carbon nanotubes. *Journal of Physica Condensed Matter*, **19**, 395017 (2007)

[8] Chen, J. H., Zhang, J., and Han, R. S. First principles calculation of transport property in nano-devices under an external magnetic field. *Chinese Physics B*, **17**, 2208–2216 (2008)

[9] Kibalchenko, M., Payne, M. C., and Yates, J. R. Magnetic response of single-walled carbon nanotubes induced by an external magnetic field. *ACS Nano*, **5**, 537–545 (2011)

[10] Roche, S. and Saito, R. Effects of magnetic field and disorder on the electronic properties of carbon nanotubes. *Physical Review B*, **59**, 5242–5246 (1999)

[11] Lobo, T., Figureira, M. S., Latgé, A., and Ferreira, M. S. Magnetic-field effects on the electronic transport properties of a carbon nanotube with a side-coupled magnetic impurity. *Physica B-Condensed Matter*, **384**, 113–115 (2006)

[12] Zhang, Z. H., Guo, W. L., and Guo, Y. F. The effects of axial magnetic field on electronic properties of carbon nanotubes. *Acta Physica Sinica*, **55**, 6526–6531 (2006)

[13] Sebastiani, D. and Kudin, K. N. Electronic response properties of carbon nanotubes in magnetic fields. *ACS Nano*, **2**, 661–668 (2008)

[14] Kibis, O. V. Electronic phenomena in chiral carbon nanotubes in the presence of a magnetic field. *Physica E-Low-Dimensional Systems and Nanostructures*, **12**, 741–744 (2002)

[15] Wang, H., Dong, K., Men, F., Yan, Y. J., and Wang, X. Influences of longitudinal magnetic field on wave propagation in carbon nanotubes embedded in elastic matrix. *Applied Mathematical Modelling*, **34**, 878–889 (2010)

[16] Narendar, S., Gupta, S. S., and Gopalakrishnan, S. Longitudinal magnetic field effect on nonlocal ultrasonic vibration analysis of single-walled carbon nanotubes based on wave propagation approach. *Advance Science Letters*, **4**, 3382–3389 (2011)

[17] Li, S., Xie, H. J., and Wang, X. Dynamic characteristics of multi-walled carbon nanotubes under a transverse magnetic field. *Bulletin Material Science*, **34**, 45–52 (2011)

[18] Narendar, S., Gupta, S. S., and Gopalakrishnan, S. Wave propagation in single-walled carbon nanotube under longitudinal magnetic field using nonlocal Euler-Bernoulli beam theory. *Applied Mathematical Modelling*, **36**, 4529–4538 (2012)

[19] Wang, X., Shen, J. X., Liu, Y., Shen, G. G., and Lu, G. Rigorous van der Waals effect on vibration characteristics of multi-walled carbon nanotubes under a transverse magnetic field. *Applied Mathematical Modelling*, **36**, 648–656 (2012)

[20] Kiani, K. Transverse wave propagation in elastically confined single-walled carbon nanotubes subjected to longitudinal magnetic fields using nonlocal elasticity models. *Physica E-Low-Dimensional Systems and Nanostructures*, **45**, 86–96 (2012)

[21] Kiani, K. Magneto-elastio-dynamic analysis of an elastically confined conducting nanowire due to an axial magnetic shock. *Physics Letters A*, **376**, 1679–1685 (2012)

[22] Murmu, T., McCarthy, M. A., and Adhikari, S. Nonlocal elasticity based magnetic field affected vibration response of double single-walled carbon nanotube systems. *Journal of Applied Physics*, **111**, 113511 (2012)

[23] Wang, B., Deng, Z., Ouyang, H., and Zhang, K. Wave characteristics of single-walled fluid-conveying carbon nano-tubes subjected to multi-physical fields. *Physica E-Low-Dimensional Systems and Nanostructures*, **52**, 97–105 (2013)

[24] Kiani, K. Vibration and instability of single-walled carbon nanotube in a three-dimensional magnetic field. *Journal of Physical and Chemical Solids*, **75**, 15–22 (2014)

[25] Rao, S. R. *Vibration of Continuous Systems*, John Wiley & Sons, New Jersey (2007)

[26] Love, A. E. H. *A Treatise on the Mathematical Theory of Elasticity*, Dover Publications, New York (1944)

[27] Eringen, A. C. *Nonlocal Continuum Field Theories*, Springer-Verlag, New York (2002)

[28] Altan, B. and Aifantis, E. C. On the structure of the mode III crack-tip in gradient elasticity. *Scripta Metallurgica et Materialia*, **26**, 319–324 (1992)

[29] Gutkin, M. Y. and Aifantis, E. C. Screw dislocation in gradient elasticity. *Scripta Materialia*, **36**, 129–135 (1996)

[30] Gutkin, M. Y. and Aifantis, E. C. Dislocations and disclinations in gradient elasticity. *Physica Status Solidi B-Basic Solid State Physics*, **214**, 245–284 (1999)

[31] Gutkin, M. Y. and Aifantis, E. C. Dislocations in the theory of gradient elasticity. *Scripta Materialia*, **40**, 559–566 (1999)

[32] Aifantis, E. C. Update on a class of gradient theories. *Mechanics of Materials*, **35**, 259–280 (2003)

[33] Song, J., Shen, J., and Li, X. F. Effects of initial axial stress on wave propagating in carbon nanotubes using a generalized nonlocal model. *Computational Material Science*, **49**, 518–523 (2010)

[34] Shen, J., Wu, J. X., Song, J., Li, X. F., and Lee, K. Y. Flexural waves of carbon nanotubes based on generalized gradient elasticity. *Physica Status Solidi B-Basic Solid State Physics*, **249**, 50–57 (2012)

[35] Challamel, N., Rakotomanana, L., and Marrec, L. L. A dispersive wave equation using nonlocal elasticity. *Comptes Rendus Mecanique*, **337**, 591–595 (2009)

[36] Kecs, W. W. A generalized equation of longitudinal vibrations for elastic rods: the solution and uniqueness of a boundary initial value problem. *European Journal of Mechanics A-Solids*, **13**, 135–145 (1994)

[37] Güven, U. The investigation of the nonlocal longitudinal stress waves with modified couple stress theory. *Acta Mechanica*, **221**, 321–325 (2011)

[38] Güven, U. A more general investigation for the longitudinal stress waves in microrods with initial stress. *Acta Mechanica*, **223**, 2065–2074 (2012)

[39] Güven, U. Love-Bishop rod solution based on strain gradient elasticity theory. *Comptes Rendus Mecanique*, **342**, 8–16 (2014)

[40] Güven, U. A generalized nonlocal elasticity solution for the propagation of longitudinal stress waves in bars. *European Journal of Mechanics A-Solids*, **45**, 75–79 (2014)

[41] Güven, U. Two mode Mindlin-Herrmann rod solutions based on strain gradient elasticity theory. *Zeitschrift für Angewandte Mathematik und Mechanik*, **94**, 1011–1016 (2014)

[42] Narendar, S. Tera hertz wave propagation in uniform nanorods: a nonlocal continuum mechanics formulation including the effect of lateral inertia. *Physica E-Low-Dimensional Systems and Nanostructures*, **43**, 1015–1020 (2011)

[43] Wang, Y. Z., Li, F. M., and Kishimoto, K. Scale effects on the longitudinal wave propagation in nanoplates. *Physica E-Low-Dimensional Systems and Nanostructures*, **42**, 1356–1360 (2010)

[44] Sanchez-Portal, D., Artacho, E., and Soler, J. M. Ab initio structural, elastic, and vibrational properties of carbon nanotubes. *Physical Review B*, **59**, 12678–12688 (1999)